

***Electronic Supplementary Information***

General approach to construct hierarchical-structured porous Co-Ni bimetallic oxide for efficient oxygen evolution

*Ping Li,<sup>\*a,b</sup> Ran Chen,<sup>a,b</sup> Yunan Lin<sup>a,b</sup> and Wenqin Li<sup>a,b</sup>*

<sup>a</sup> School of Environmental Science and Engineering, Sun Yat-sen University, Guangzhou 510275, Guangdong, P. R. China.

<sup>b</sup> Guangdong Provincial Key Laboratory of Environmental Pollution Control and Remediation Technology, Guangzhou 510275, P. R. China.

E-mail: liping56@mail.sysu.edu.cn

**Table of Contents**

Figures S1 to S11 .....	Pages 2-8
Table S1 .....	Pages 9-10
References .....	Pages 10-12

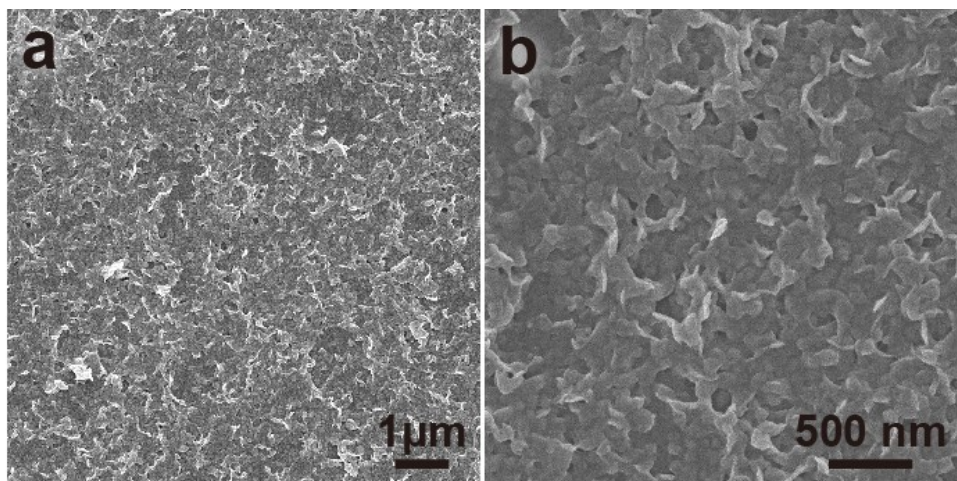


**Figure S1.** (a,b) SEM images of the CoNi-DiEG prepared by using pure DiEG as solvent without adding methanol.

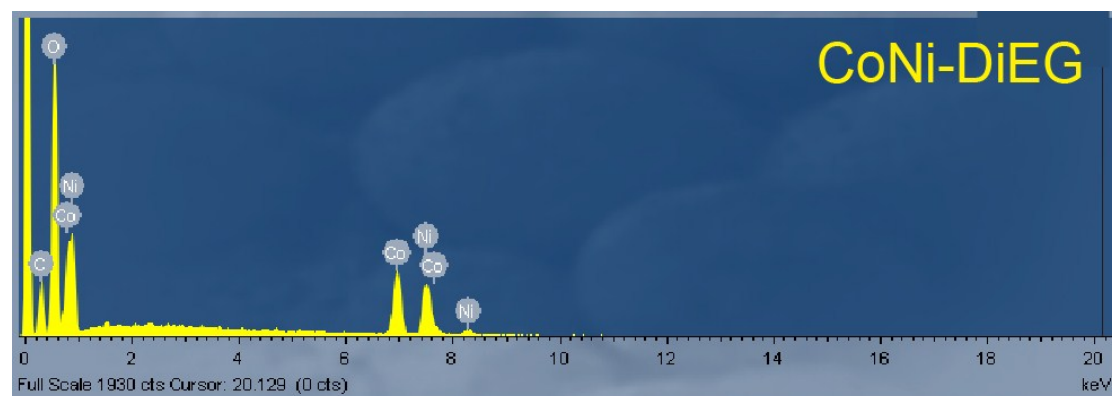


**Figure S2.** The EDX spectrum of the CoNi-DiEG precursor.

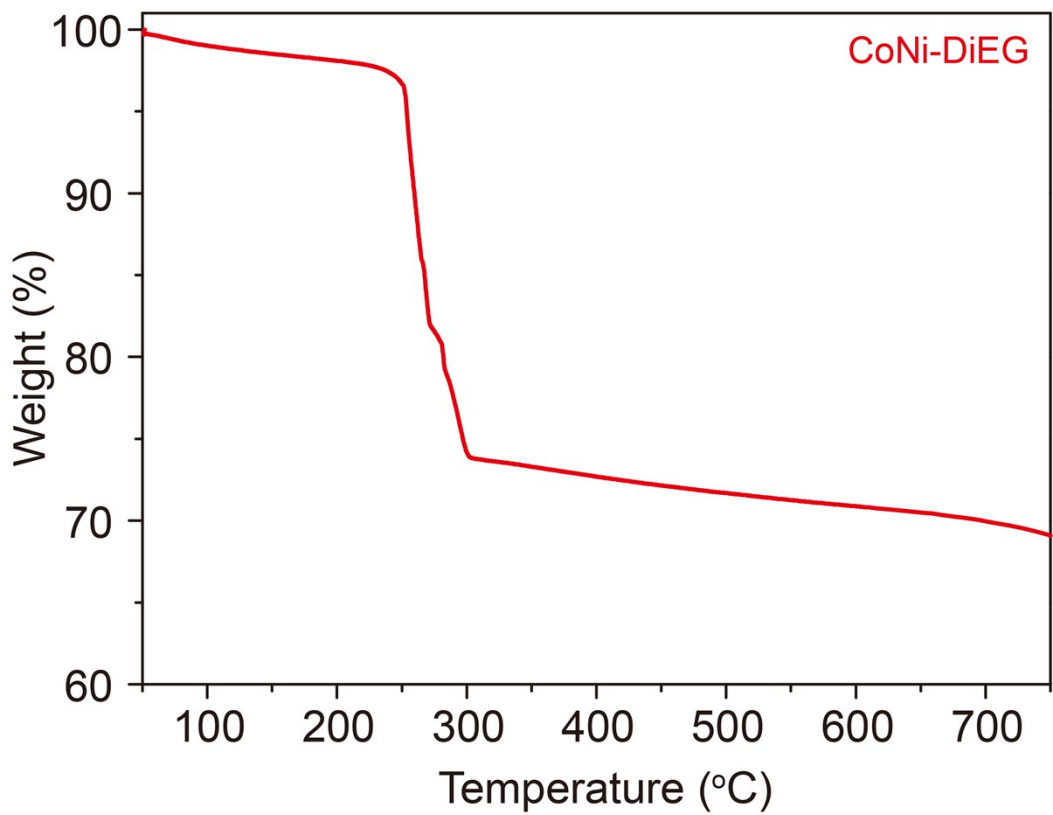


**Figure S3.** The TGA curve of the CoNi-DiEG precursor.

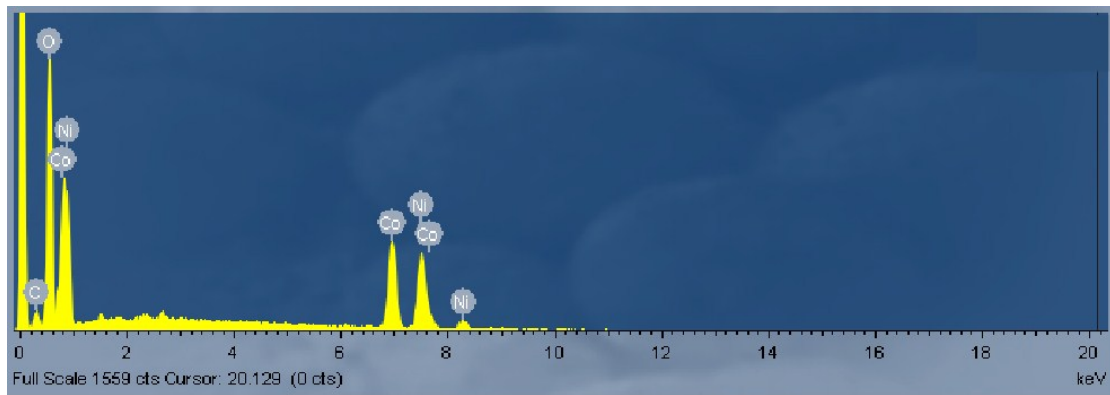


**Figure S4.** The EDX spectrum of the  $\text{CoNiO}_x$ .

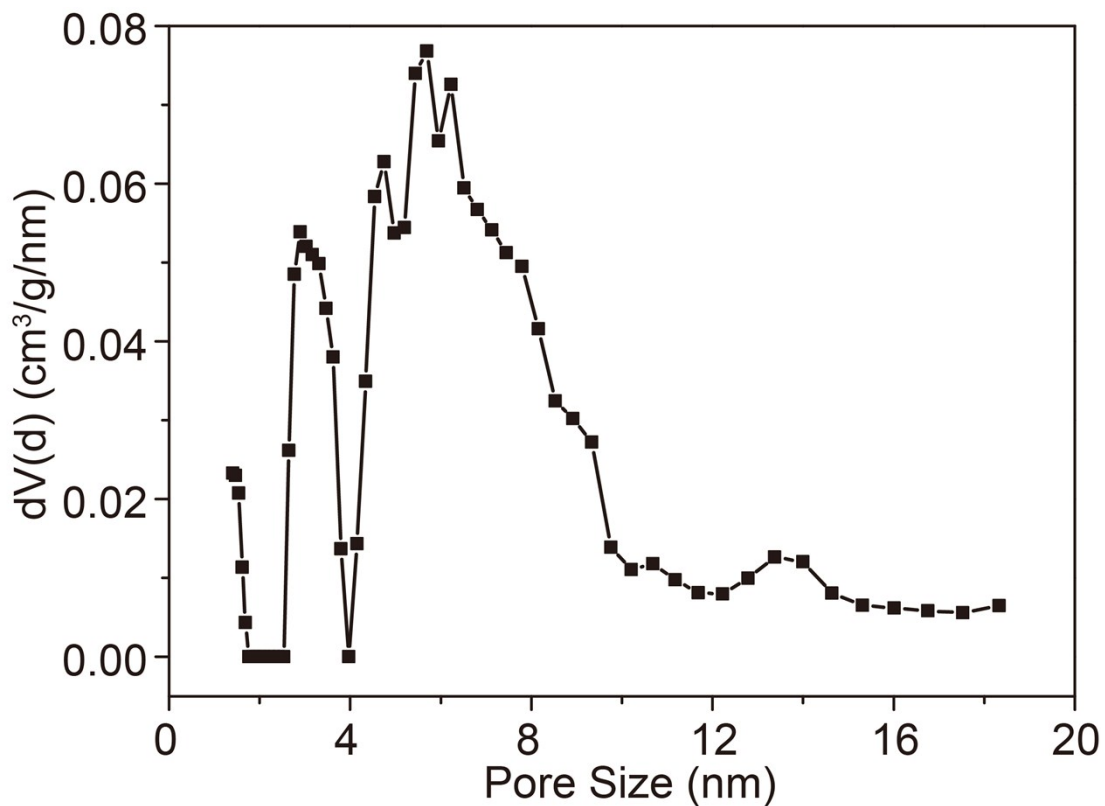


**Figure S5.** The NLDFT pore size distribution curve of the CoNiO<sub>x</sub>.

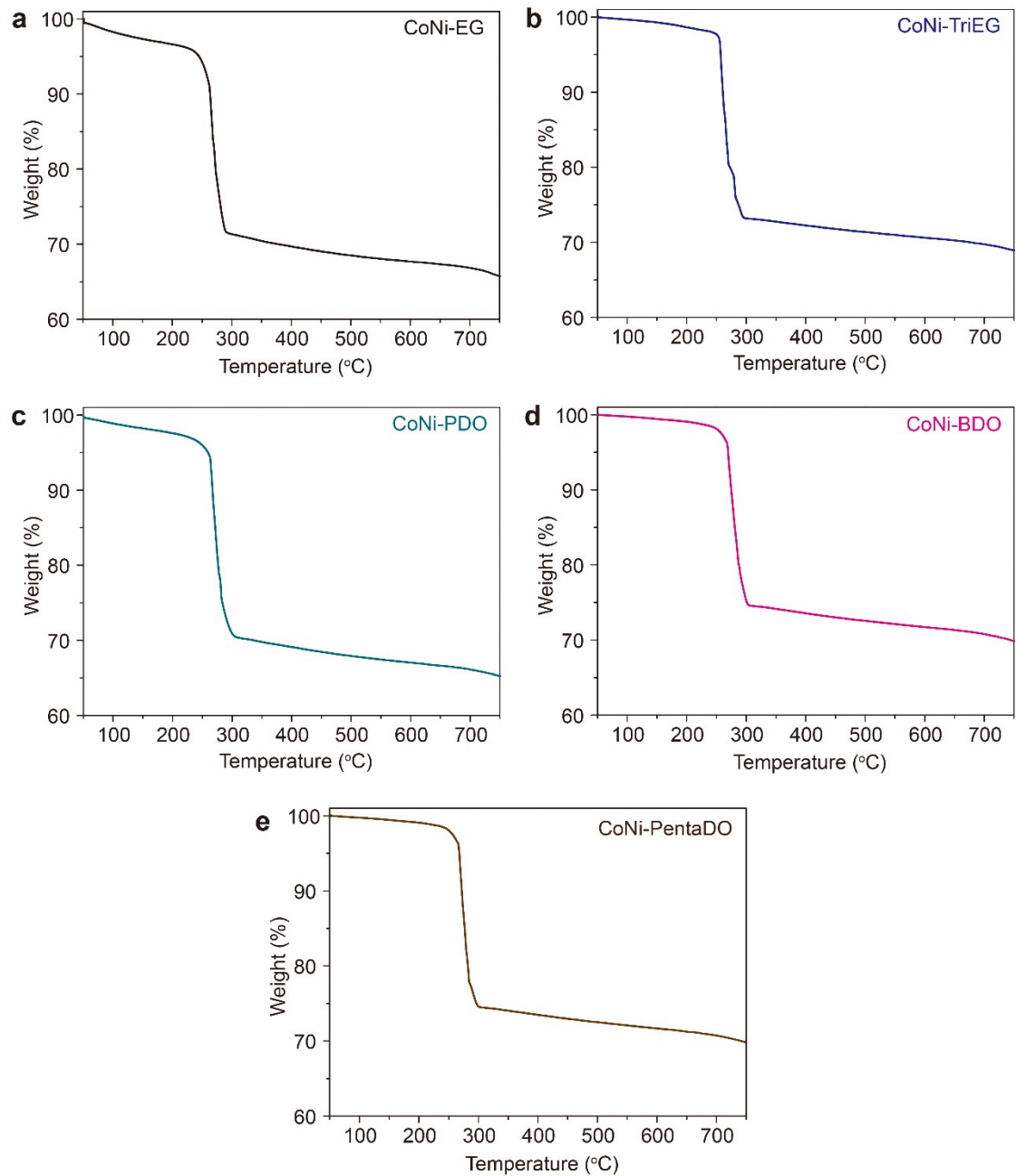


**Figure S6.** The TGA curves of various CoNi-polyol complexes: (a) CoNi-EG, (b) CoNi-TriEG, (c) CoNi-PDO, (d) CoNi-BDO, and (e) CoNi-PentaDO.

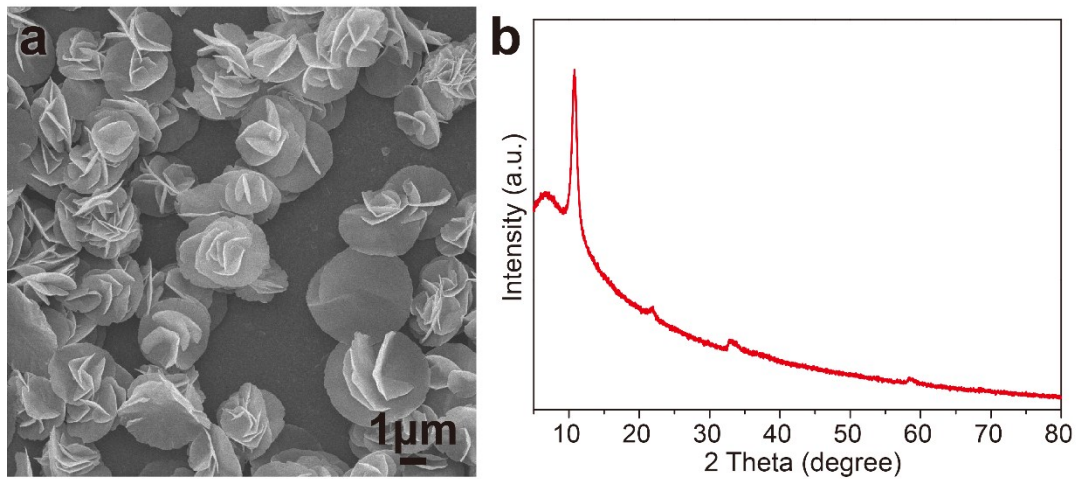


**Figure S7.** Characterizations of Co-DiEG precursor: (a) SEM image and (b) XRD pattern.

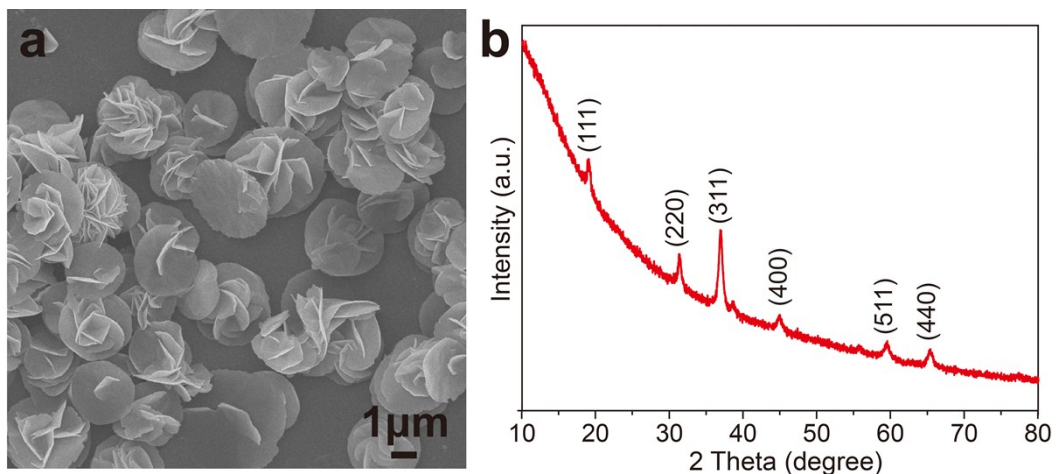


**Figure S8.** Characterizations of  $\text{Co}_3\text{O}_4$ : (a) SEM image and (b) XRD pattern.

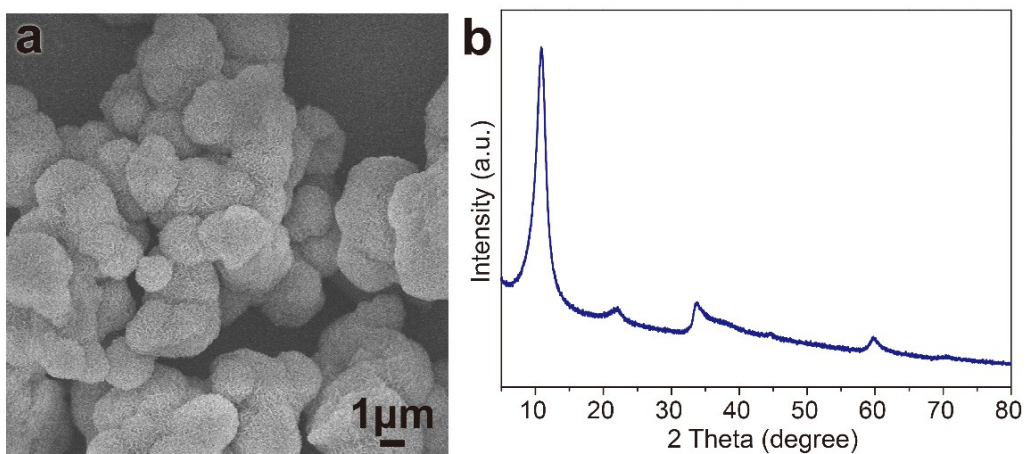


**Figure S9.** Characterizations of Ni-DiEG precursor: (a) SEM image and (b) XRD pattern.

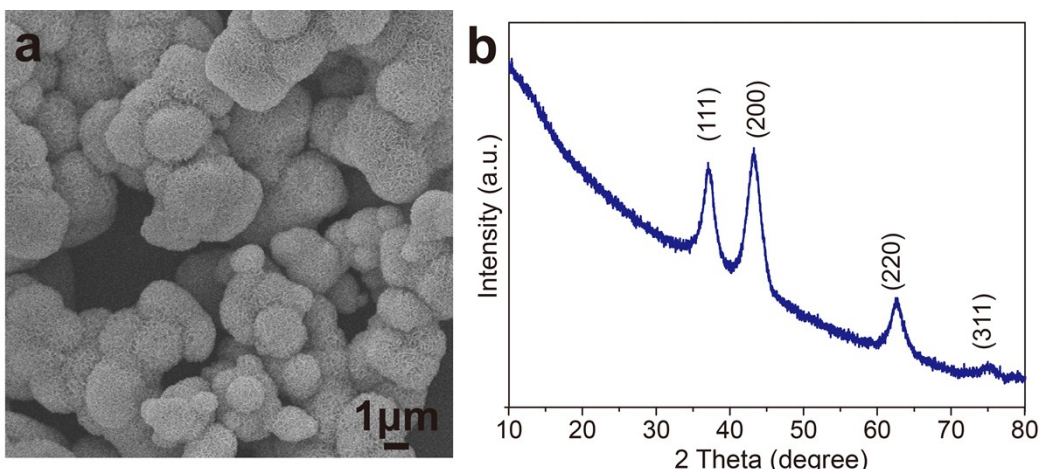


**Figure S10.** Characterizations of NiO: (a) SEM image and (b) XRD pattern.

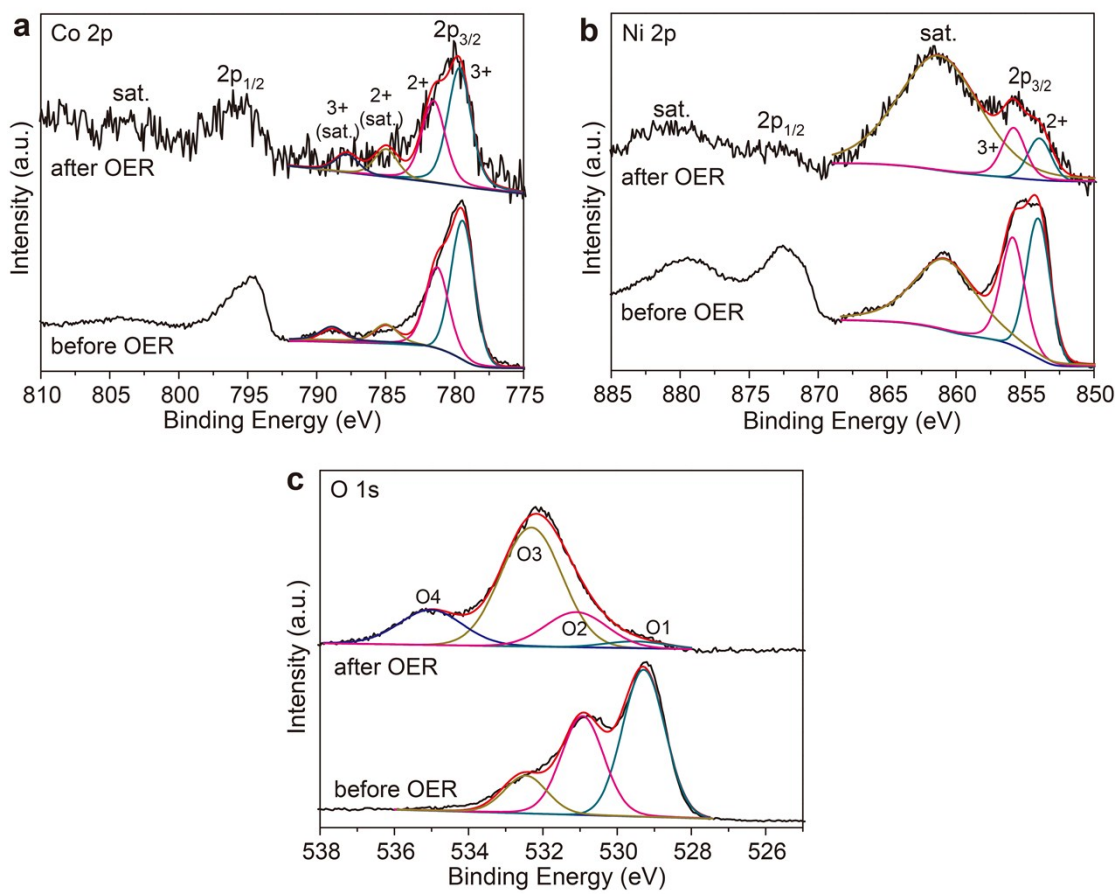


**Figure S11.** (a) Co 2p, (b) Ni 2p, and (c) O 1s XPS spectra of the CoNiO<sub>x</sub> before and after the electrochemical CP stability test.

**Notes:** For the XPS spectra of the CoNiO<sub>x</sub>, the Co 2p (Figure S11a) and Ni 2p spectra (Figure S11b) are split into 2p<sub>3/2</sub> and 2p<sub>1/2</sub> doublets, due to the spin-orbit coupling, together with shakeup satellite peaks. And both Co 2p<sub>3/2</sub> and Ni 2p<sub>3/2</sub> spectra can be deconvoluted into two distinct metal species, i.e., Co<sup>2+</sup> (781.3 eV) and Co<sup>3+</sup> (779.4 eV), Ni<sup>2+</sup> (854.2 eV) and Ni<sup>3+</sup> (855.9 eV), indicating the coexistence of Co<sup>2+</sup>, Co<sup>3+</sup>, Ni<sup>2+</sup> and Ni<sup>3+</sup> in the sample.<sup>1</sup> In the O 1s spectrum (Figure S11c), three peaks can be clearly identified. The peak at ~529.3 eV is attributed to the lattice oxygen in the spinel oxide, the peak at ~530.9 eV is assigned to the surface defect sites with a low oxygen coordination, and the peak at ~532.5 eV can be assigned to the hydroxyl species.<sup>2,3</sup>

**Table S1.** Comparison of the OER catalytic performance of our hierarchical-structured porous CoNiO<sub>x</sub> to other recently reported high-performance OER catalysts in alkaline solution.

Catalyst	Mass loading (mg cm <sup>-2</sup> )	Electrolyte	η@10 mA cm <sup>-2</sup> (mV)	Tafel slope (mV dec <sup>-1</sup> )	Ref.
<b>CoNiO<sub>x</sub></b>	<b>0.2</b>	<b>0.1 M KOH</b>	<b>329 309 (after CP test)</b>	<b>66</b>	<b>this work</b>
α-Ni(OH) <sub>2</sub> spheres	0.2	0.1 M KOH	331	42	4
β-Ni(OH) <sub>2</sub> plates	0.2	0.1 M KOH	444	111	4
Hollow Co <sub>3</sub> S <sub>4</sub> nanosheets	0.283	0.1 M KOH	363	90	5
Mn <sub>3</sub> O <sub>4</sub> /CoSe <sub>2</sub>	0.2	0.1 M KOH	450	49	6
N-graphene-CoSe <sub>2</sub>	0.2	0.1 M KOH	366	40	7
N-Co <sub>9</sub> S <sub>8</sub> /graphene	0.2	0.1 M KOH	409	82.7	8
Co <sub>3</sub> O <sub>4</sub> /C nanowire arrays	0.2	0.1 M KOH	290	70	9
Ordered mesoporous Co <sub>3</sub> O <sub>4</sub>	0.12	0.1 M KOH	496-537	86-96	10
Ba <sub>0.5</sub> Sr <sub>0.5</sub> Co <sub>0.8</sub> Fe <sub>0.2</sub> O <sub>3-d</sub>	0.25	0.1 M KOH	362	48	11
FeNC sheets/NiO	0.24	0.1 M KOH	390	76	12
CoNC sheets/NiO	0.24	0.1 M KOH	410	80	12
Ultrathin NiCo <sub>2</sub> O <sub>4</sub> nanosheets	0.285	0.1 M KOH	415	N.A.	2
rGO@CoNiO <sub>x</sub>	0.2	0.1 M KOH	320	45	3
NiFe-LDH/CNTs	0.2	0.1 M KOH	308	35	13
sea-urchin-like (Co <sub>0.54</sub> Fe <sub>0.46</sub> )P <sub>2</sub>	0.2	0.1 M KOH	370	N.A.	14
Ag-CoSe <sub>2</sub> nanobelts	0.2	0.1 M KOH	320	56	15

N-doped graphitic carbon	0.2	0.1 M KOH	380	75-80	16
P-doped graphitic C <sub>3</sub> N <sub>4</sub>	0.2	0.1 M KOH	400	61.6	17
Graphitic C <sub>3</sub> N <sub>4</sub> nanosheets/carbon nanotubes	0.2	0.1 M KOH	370	83	18
IrO <sub>2</sub> /C	0.2	0.1 M KOH	370	N.A.	16
Rutile RuO <sub>2</sub>	0.05	0.1 M KOH	> 470	N.A.	19
RuO <sub>2</sub> /C	0.2	0.1 M KOH	380	157.5	8
RuO <sub>2</sub>	0.2	0.1 M KOH	387	90	4
Ni <sub>x</sub> Co <sub>3-x</sub> O <sub>4</sub> nanowire arrays	2.3-2.7	1 M NaOH	370	59-64	20
Ni-Co oxide hierarchical nanosheets	N.A.	1 M NaOH	340	51	21
Amorphous NiCo <sub>2.7</sub> (OH) <sub>x</sub> nanocages	0.2	1 M KOH	350	65	22
NiCo LDH nanosheets	0.17	1 M KOH	367	40	23
rGO/CoNi-P	0.1	1 M KOH	314	60.0	24
CoP/NCNHP	N.A.	1 M KOH	310	70	25
CoP/rGO	0.28	1 M KOH	340	66	26

### References:

- I. Abidat, N. Bouchenafa-Saib, A. Habrioux, C. Comminges, C. Canaff, J. Rousseau, T. W. Napporn, D. Dambouronet, O. Borkiewicz and K. B. Kokoh, *J. Mater. Chem. A*, 2015, **3**, 17433-17444.
- J. Bao, X. Zhang, B. Fan, J. Zhang, M. Zhou, W. Yang, X. Hu, H. Wang, B. Pan and Y. Xie, *Angew. Chem. Int. Ed.*, 2015, **54**, 7399-7404.

3. P. Li and H. C. Zeng, *Adv. Funct. Mater.*, 2017, **27**, 1606325.
4. M. Gao, W. Sheng, Z. Zhuang, Q. Fang, S. Gu, J. Jiang and Y. Yan, *J. Am. Chem. Soc.*, 2014, **136**, 7077-7084.
5. W. Zhao, C. Zhang, F. Geng, S. Zhuo and B. Zhang, *ACS Nano*, 2014, **8**, 10909-10919.
6. M.-R. Gao, Y.-F. Xu, J. Jiang, Y.-R. Zheng and S.-H. Yu, *J. Am. Chem. Soc.*, 2012, **134**, 2930-2933.
7. M.-R. Gao, X. Cao, Q. Gao, Y.-F. Xu, Y.-R. Zheng, J. Jiang and S.-H. Yu, *ACS Nano*, 2014, **8**, 3970-3978.
8. S. Dou, L. Tao, J. Huo, S. Wang and L. Dai, *Energy Environ. Sci.*, 2016, **9**, 1320-1326.
9. T. Y. Ma, S. Dai, M. Jaroniec and S. Z. Qiao, *J. Am. Chem. Soc.*, 2014, **136**, 13925-13931.
10. X. Deng, W. N. Schmidt and H. Tüysüz, *Chem. Mater.*, 2014, **26**, 6127-6134.
11. J. Suntivich, K. J. May, H. A. Gasteiger, J. B. Goodenough and Y. Shao-Horn, *Science*, 2011, **334**, 1383-1385.
12. J. Wang, K. Li, H.-x. Zhong, D. Xu, Z.-l. Wang, Z. Jiang, Z.-j. Wu and X.-b. Zhang, *Angew. Chem. Int. Ed.*, 2015, **54**, 10530-10534.
13. M. Gong, Y. Li, H. Wang, Y. Liang, J. Z. Wu, J. Zhou, J. Wang, T. Regier, F. Wei and H. Dai, *J. Am. Chem. Soc.*, 2013, **135**, 8452-8455.
14. A. Mendoza-Garcia, H. Zhu, Y. Yu, Q. Li, L. Zhou, D. Su, M. J. Kramer and S. Sun, *Angew. Chem. Int. Ed.*, 2015, **54**, 9642-9645.
15. X. Zhao, H. Zhang, Y. Yan, J. Cao, X. Li, S. Zhou, Z. Peng and J. Zeng, *Angew. Chem. Int. Ed.*, 2017, **56**, 328-332.
16. Y. Zhao, R. Nakamura, K. Kamiya, S. Nakanishi and K. Hashimoto, *Nat Commun*, 2013, **4**, 2390.
17. T. Y. Ma, J. Ran, S. Dai, M. Jaroniec and S. Z. Qiao, *Angew. Chem. Int. Ed.*, 2015, **54**, 4646-4650.
18. T. Y. Ma, S. Dai, M. Jaroniec and S. Z. Qiao, *Angew. Chem. Int. Ed.*, 2014, **53**,

7281-7285.

19. Y. Lee, J. Suntivich, K. J. May, E. E. Perry and Y. Shao-Horn, *J. Phys. Chem. Lett.*, 2012, **3**, 399-404.
20. Y. Li, P. Hasin and Y. Wu, *Adv. Mater.*, 2010, **22**, 1926-1929.
21. H.-Y. Wang, Y.-Y. Hsu, R. Chen, T.-S. Chan, H. M. Chen and B. Liu, *Adv. Energy Mater.*, 2015, **5**, 1500091.
22. J. Nai, H. Yin, T. You, L. Zheng, J. Zhang, P. Wang, Z. Jin, Y. Tian, J. Liu, Z. Tang and L. Guo, *Adv. Energy Mater.*, 2015, **5**.
23. H. Liang, F. Meng, M. Cabán-Acevedo, L. Li, A. Forticaux, L. Xiu, Z. Wang and S. Jin, *Nano Lett.*, 2015, **15**, 1421-1427.
24. P. Li and H. C. Zeng, *ACS Appl. Mater. Interfaces*, 2019, **11**, 46825-46838.
25. Y. Pan, K. Sun, S. Liu, X. Cao, K. Wu, W.-C. Cheong, Z. Chen, Y. Wang, Y. Li, Y. Liu, D. Wang, Q. Peng, C. Chen and Y. Li, *J. Am. Chem. Soc.*, 2018, **140**, 2610-2618.
26. L. Jiao, Y.-X. Zhou and H.-L. Jiang, *Chem. Sci.*, 2016, **7**, 1690-1695.